

We are IntechOpen, the world's leading publisher of Open Access books Built by scientists, for scientists

6,900

Open access books available

185,000

International authors and editors

200M

Downloads

Our authors are among the

154

Countries delivered to

TOP 1%

most cited scientists

12.2%

Contributors from top 500 universities



WEB OF SCIENCE™

Selection of our books indexed in the Book Citation Index
in Web of Science™ Core Collection (BKCI)

Interested in publishing with us?
Contact book.department@intechopen.com

Numbers displayed above are based on latest data collected.
For more information visit www.intechopen.com



Modeling of Creep Deformation and Creep Fracture

Qiang Xu and Zhongyu Lu

Abstract

This chapter reports the recent progresses in (1) the development of a modified hyperbolic sine law able to depict the minimum creep strain rate over a wider range of stress levels; (2) the development of the creep fracture criterion and model based on the cavity area fraction along grain boundary calibrated with the most representative and comprehensive cavitation data obtained from X-ray synchrotron investigation; and (3) the development of mesoscopic composite approach modeling of creep deformation and creep damage. The first progress facilitates to overcome the difficulty in creep deformation modeling caused by stress breakdown phenomenon; the second progress is of a really scientifically sound and fundamental new approach, first in the world; the third progress provides the concept and tool, at the appropriate size scale, for the modeling of the creep deformation and creep fracture. They all contribute to the specific knowledge and new methodology to the topic area. Furthermore, it is expected that cavitation fracture modeling methodology reported here will find use in the analysis and modeling of other types of failure such as ductile and fatigue failure. This chapter presents an excellent example of interdisciplinary collaborative research and it advocates further such collaboration in its conclusion.

Keywords: creep stress breakdown, creep strain and stress law, Xu's modified hyperbolic sine law, creep cavitation damage and fracture model, X-ray synchrotron cavitation; mesoscopic composite type modeling

1. Introduction

1.1 General

Creep damage is one of the life-limiting factors for high-temperature components. A sound scientific understanding and an accurate mathematical description of the creep deformation and creep fracture are of great interest to and a challenge for the materials and structural integrity research communities and high-temperature industries.

It is generally understood and accepted that for the majority of metals and alloys, creep cavitation at grain boundary is the cause for the creep fracture [1, 2].

Creep continuum damage mechanics (CDM) has been developed to model creep deformation and creep fracture, where internal variables were introduced to depict the macroscopic behavior and the cavitation is incorporated in an average, smeared-out manner.

High Cr alloys is one of the alloys developed for and utilized in power generation industry. So, they have been chosen for the research, and progress made with them will be reported here. Additionally, copper-antimony alloy is used in the illustrative example of the mesoscopic composite modeling of creep deformation and fracture due to the unavailability of the micro-mechanical constitutive equation for high Cr alloys. Although the examples of progress reported here are based on the specific material, the methodology is generic and not material dependent.

1.2 The problem

In the development of and particularly in the characterization of high-temperature structural materials, the accelerated creep testing (short-term) may be conducted; then the result might be extrapolated for long-term service condition (say 100,000 hours). Normally, this approach is not reliable, as this microstructure may progressively degrade with often unexpected consequences for long-term creep performance under lower applied stress. Such phenomenon is called stress breakdown; it profoundly exists in high Cr alloys [3–7].

Ennis et al. [3] found that the Norton stress exponent n was found to be 16 for the stresses of above 150 MPa at 600°C and above 110 MPa for 650°C, and an n value was 6 below these stresses. A selection of quantitative presentation of the dependence of the minimum creep strain rate, creep lifetime, and strain at failure on the stress level can be found in [3]. Furthermore, Lee et al. [4] found (1) the stress exponent for rupture life to be decreased from 17 in short-term creep to 8 in long-term creep for the ASTM grade 92 steel crept at 550–650°C for up to 63,151 h, (2) the change of fracture mechanisms with stress level, and (3) creep cavities nucleated at coarse precipitates of Laves phase along grain boundaries.

It can be seen that (1) a wider range of stresses, particularly the lower stress level, must be considered; (2) there is a change of creep deformation mechanism and possible creep damage mechanism under the different stress level. Currently, there is no adequate and accurate data to characterize the creep cavity nucleation, growth, and coalescence under lower stress.

1.3 Current creep cavity damage modeling

In an attempt to model the long-term creep behavior, Yin et al. [8] have proposed a phenomenological relationship between the creep cavity damage and creep strain, which departed from the firm and well-known mechanism-based relationship of Dyson [9]. The relevant equations are listed below for completeness:

Dyson [9]:

$$\dot{D}_n = \frac{k_N}{\varepsilon_{f_u}} \dot{\varepsilon} \quad (1)$$

Yin et al. [8]:

$$\dot{D}_n = A \varepsilon^{B'} \dot{\varepsilon} \quad (2)$$

where A is the creep cavity damage coefficient, and it is assumed that it does not change with stress, it changes with temperature.

Yin's approach cannot be extrapolated into a lower stress level than it has been calibrated according to Yang et al. [10] as a constant value of A is not able to depict the stress breakdown phenomenon.

Basirat et al. followed Yin's approach but allowed the cavity damage coefficient to be stress level dependent, in the following form [11]:

$$\dot{D}_n = A\dot{\epsilon}\epsilon^{0.9} \quad (3)$$

However, an unexpected abnormal variation of the value of A with stress level occurred which is shown in **Table 1** and graphically in **Figure 1** [12]. Due to the lack of a trend with stress level, it is hard to use them in prediction with confidence. The concept of creep cavity damage coefficient to be stress level dependent had been introduced by the first author in 2003 [13] for low Cr alloy creep damage modeling where no such abnormality occurred.

Hence, the phenomenological modeling of creep cavity damage for high Cr alloy is not satisfactory.

Furthermore, the methodology, based on the isochronous surface concept only, for the generalization of a set of uniaxial creep damage constitutive equations into a set of multiaxial version is conceptually flawed [14–16]. Though the creep deformation consistence has to be included, this has not been very well appreciated by the majority of research community, even in the published review type of articles. Progress can be found only in very limited publications, for example, the original one [16, 17] and the more recent one [18].

1.4 Opportunity and research progress

1. Examination and development of the law of the minimum creep strain rate and a wider range of stress levels. The development and application of Xu's modified hyperbolic sine law will be reported with an illustrative example.
2. Modeling of creep cavity damage and creep cavity fracture.

Parameter	$\sigma = 80\text{MPa}$	$\sigma = 100\text{MPa}$	$\sigma = 150\text{MPa}$	$\sigma = 200\text{MPa}$	Temperatures(°C)
A	57	83	1	112	600
A	57	83	47	145	650
A	57	83	113	146	700

Table 1.
 The variation of cavitation coefficient A [11].

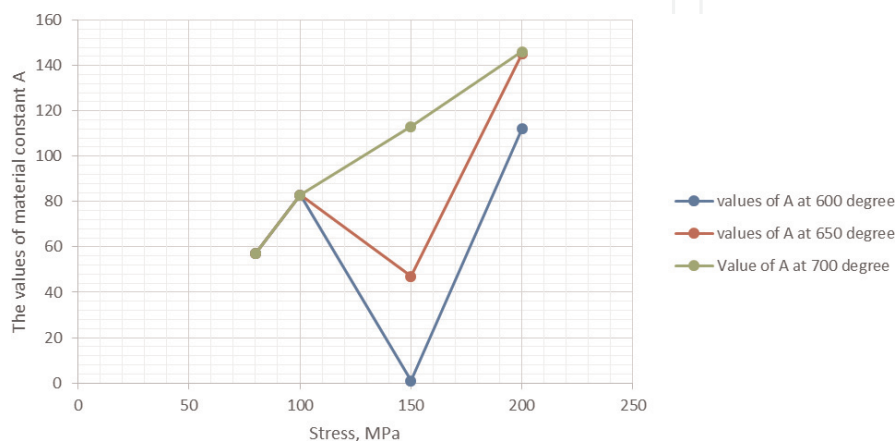


Figure 1.
 The variation of creep cavity damage coefficient A with different stress and temperature [12].

In 2013, the first author noted that the available creep cavitation data is produced with X-ray synchrotron technique by materials scientists. The X-ray synchrotron is a very advanced technique, and it is able to produce a detail and un-destructive, hence more presentative, information over a small volume. This is a very significant advance for the characterization of creep cavitation. Hence, it was the author's view [19] that such information about cavitation should be very valuable for the modeling of creep cavity damage and fracture. Such breakthrough in modeling of creep cavity damage and fracture will be reported with selected examples.

3. The mesoscopic composite approach modeling of creep deformation and damage

Furthermore, the authors [15] have observed that the current creep continuum damage mechanics operates at macroscopic level is of phenomenological suffering an ambiguity in the depicting of the creep deformation and creep cavity damage and fracture [15], hence, concluded that a mesoscopic composite approach modeling is necessary and better. In this new approach, the grain and grain boundary will be separately presented in space and in property (constitutive equations) to specifically reflect the creep deformation processes and creep damage processes and the ultimate creep fracture. The initial progress will be reported in this chapter.

4. This chapter ends with discussion, conclusion, and suggestion for future work which advocates closer interdisciplinary collaboration.

2. Methods and materials

2.1 The modified hyperbolic sine law for minimum creep strain rate and stress law

Xu's modified hyperbolic sine law is given as [12]:

$$\dot{\epsilon}_{min} = A \sinh(B\sigma^q) \quad (4)$$

It was originally proposed by the first author for low Cr alloy [12], and its application was very successful [12].

Other existing and commonly used laws for high Cr P91 are listed **Table 2**; their suitability was examined first prior to the adoption of Xu's modified law.

The specific material used here is P91 (9Cr-1Mo-V-Nb). The experimental data of the minimum creep strain rate over a range of stress levels was taken from the published creep data [20] produced by the National Institute for Materials Science (NIMS), Japan.

Power law	$\dot{\epsilon}_{min} = A\sigma^n$
Linear + power law	$\dot{\epsilon}_{min} = A\sigma[1 + (B\sigma)^n]$
Hyperbolic sine law	$\dot{\epsilon}_{min} = A \sinh(B\sigma)$
Xu' modified hyperbolic sine law	$\dot{\epsilon}_{min} = A \sinh(B\sigma^q)$

Table 2.
The list of creep laws for the minimum creep strain rate and stress.

2.2 Creep cavity fracture model

2.2.1 Method [12]

The cavitated area fraction, w , along the grain boundaries is given as [1]:

$$w = \int \pi R^2 N(R, t) dR \quad (5)$$

$$w = I(\alpha, \beta, \gamma) A_2 A_1^{\frac{2}{\beta+1}} t^{\alpha+\beta+\frac{(1-\alpha)(\beta+3)}{\beta+1}} \quad (6)$$

where the dimensionless factor $I(\alpha, \beta, \gamma)$ is definite integral

$$I = \pi(1 + \beta)^{(\beta+3)/(\beta+1)} \int_0^U x^{\beta+2} [1 - (1 - \alpha)x^{\beta+1}]^{(\alpha+\beta)/(1-\alpha)} dx \quad (7)$$

and the cavity size distribution function, $N(R, t)$, represents the number of voids with radii between R and $+dR$ in the time interval t and $t + dt$:

$$N(R, t) = \frac{A_2}{A_1} R^\beta t^{\alpha+\gamma} \left(1 - \frac{1 - \alpha}{1 + \beta} \frac{R^{\beta+1}}{A_1 t^{1-\alpha}} \right)^{(\alpha+\gamma)/(1-\alpha)} \quad (8)$$

if the non-station growth rate of the cavity radius and the nucleation rate of cavity are:

$$\dot{R} = A_1 R^{-\beta} t^{-\alpha} \quad (9)$$

$$J^* = A_2 t^\gamma \quad (10)$$

where the unknown constants A_1 , A_2 , α , β , and γ are material cavitation constants.

It is emphasized and concluded here that (1) if the values of creep cavitation constants A_1 , A_2 , α , β , and γ are known, the cavitated area fraction, w , could be determined quantitatively and (2) a critical value for $w_f = \frac{\pi}{4}$ for coalesce could be used as fracture criterion.

2.2.2 Determination of cavitation constants

The method for the determination of the material cavitation constants, A_1 , A_2 , α , β , and γ , depends on the available experimental cavitation data [12].

The nucleation rate and growth rate can be directly determined if such data is directly available.

Based on qualitative analysis for 3D tomographic reconstructions of the distribution voids of E911 and P91 steel, a theoretically derived function of taking into account nucleation and growth of voids [1] was used to evaluate the experimental obtained histograms; the distribution equation (8) proposed by Riedel fitted well with the histogram density functions of void equivalent radius R of E911 and P91 [21], while the identical value of $\beta = 1.95 \pm 0.05$ (closely to 2) is characterized for the constrained diffusional mechanism of void growth and $\alpha = 1$ characterized for continuum cavity nucleation [21, 22].

Cavity histogram is often used by material scientists, and it can be used to determine the values of these five or part of these constants, through either optimization method or trial and error method.

2.2.3 Explicit creep cavity damage fracture model

The explicit creep fracture model can be derived with the given values of creep cavitation constants [12].

For the given values of $\alpha = 1, \beta = 2$, and $\gamma = 1$ for P91 [12], Eq. (5), w , is simplified as:

$$w = \pi \times \frac{3}{5} \times 3^{\frac{2}{3}} \times U^5 \times A_1^{2/3} A_2 \times t^{1+\gamma} \quad (11)$$

And further,

$$w = U' \times t^{1+\gamma} \quad (12)$$

where $U' = \pi \times \frac{3}{5} \times 3^{\frac{2}{3}} \times U^5 \times A_1^{2/3} A_2$; it is termed as creep lifetime coefficient. Insert $\gamma = 1$ in Eq. (12); the creep cavity damage function is:

$$w = U' \times t^2 \quad (13)$$

$$w_f = U' \times t_f^2 \quad (14)$$

The creep fracture is assumed to occur when the area coverage attains a critical value, denoted by w_f . The critical value, w_f , will be chosen for as $w_f = \frac{\pi}{4}$, since regularly spaced round cavities touch each other if $w_f = \frac{\pi}{4}$ [1].

2.2.4 Application for lifetime prediction over a wider stress range

This section investigates such dependence on stress. The method is stated as:

1. The creep cavity fracture lifetime is fully described by Eq. (11), where the creep cavitation coefficients are deemed stress level dependent.
2. If the creep cavity coefficients are known at different stress levels, then there is a simple ratio of the two creep cavity fracture lifetimes.
3. Furthermore, if the trend of the values of the creep cavity coefficients with stress is known, then the above simple ratio relationship could be used for lifetime extrapolation.
4. Approximated method for the determination of A_1 and A_2 : If α, β , and γ are known, then the values of A_1 and A_2 can be conveniently obtained by inversely using Eqs. (9) and (10) with known total number of cavity, maximum radius of cavity, and lifetime, assuming that there is no incubation time for the cavity nucleation.

2.3 Mesoscopic composite approach modelling

2.3.1 Concept development: mesoscopic composite model

1. The current creep continuum damage mechanics operates at a macroscopic level with ambiguity in the depicting of the creep deformation and creep damage; hence a mesoscopic level composite model is necessary.

2. In the mesoscopic model, the grain and grain boundary will be separately presented in space and in constitutive equations.
3. The specific creep damage constitutive equations for the grain and grain boundary need to be developed; this, in turn, requires property characterization for grain and grain boundary separately.
4. Grain element: conventional 2d or 3D element can be directly chosen and used here. Grain boundary element: interface type of element, developed for fracture mechanics, can be chosen and used.
5. Micro-mechanics-based grain boundary model [23, 24].

This micro-mechanical-based smeared-out grain boundary element for of copper-antimony alloy [23, 24] has been chosen in the current development, as there is not that much choice. The main contents are:

1. Grain boundary nucleation: Dyson's empirical equation [25] has been consulted.
2. Cavity annihilation: probabilistic description of crack annihilation [26] has been adopted.
3. Cavity growth: constrained cavity growth model [1, 27] adopted.
4. Grain boundary sliding: Ashby viscosity model [28] adopted.
5. Creep fracture criterion when the cavity area fraction along grain boundary reached 0.5, experimentally observed by Cocks and Ashby [29]. In this model, the grain boundary sliding has been considered for the deformation, but not for the cavity nucleation.

2.3.2 Grain boundary element

The GB displacement jump at a normal direction can be obtained by the model which is developed by Markus Vöse [30]. It takes into account nucleation, growth, coalescence, and sintering of multiple cavities and can be written as (Figure 10) [30, 31]:

$$\frac{d\beta}{dt} = \frac{3\beta}{2\dot{\rho}} (\dot{\alpha}_p - \dot{\alpha}_a) + \sqrt{\dot{\rho}} \sqrt[3]{36h(\psi)\pi\beta^2} \frac{d\dot{a}}{dt}, \quad (15)$$

$$\frac{d\dot{\rho}}{dt} = \dot{\alpha}_p(1-f) - \dot{\alpha}_a \quad (16)$$

$$\dot{\alpha}_a = x_3 \cdot 8\pi\dot{\rho}^2 \dot{a} \frac{d\dot{a}}{dt}, \quad (17)$$

$$\frac{d\dot{a}}{dt} = x_1 \cdot \frac{2\dot{D}_{gb}}{h(\psi)} \frac{[1 - \dot{a}_{vip}(\dot{a}) \cdot (1 - x_2\omega)]}{\dot{a}^2 \cdot q(x_2\omega)}, \quad (18)$$

$$\omega = \sqrt[3]{\frac{9\pi\beta^2}{16h^2(\psi)}}; \dot{a} = \frac{1}{\sqrt{\dot{\rho}}} \sqrt[3]{\frac{3}{4} \frac{\beta}{h(\psi)\pi}}, \quad (19)$$

$$f = \frac{(\eta - 1)\omega}{1 - \omega}, \quad (20)$$

$$\eta = \exp \left(\left[x_4 \cdot 2\pi \tilde{D}_{gb} (\dot{a}_{tip}(\dot{a} = 1) - \dot{a}_{tip}(\dot{a})) \rho \left(\frac{d\mu^p}{dt} \right)^{-1} \right] \right) \quad (21)$$

$$\frac{d\mu^p}{dt} = \frac{\beta}{\sqrt{\rho^3}} (\dot{\alpha}_p - \dot{\alpha}_a) + \sqrt[3]{36h(\psi)\pi\beta^2} \frac{d\dot{a}}{dt}, \quad (22)$$

where

$$q(\omega) = -2\ln\omega - (3 - \omega)(1 - \omega); \dot{a}_{tip}(\dot{a}) = 2\dot{\gamma}_s \sin\psi / \dot{a} \quad (23)$$

In this equation, β is the damage variable, ρ is the cavity density, a is the average radius of the cavity, $\dot{\alpha}_p$ is the stress-dependent nucleation rate, $\dot{\alpha}_a$ is the annihilation rate, ψ is the dihedral angle of the cavity (70°), \tilde{D}_{gb} is the GB diffusion coefficient, and ω is the damaged area fraction. The creep degradation of GB is calibrated by three variables: ρ , β and a . These three parameters not only determine the failure degree of GB but also determine the amount of the creep nonlinear deformation. Therefore, ρ , β , and a are the three indicators for the benchmark.

2.3.3 Computational platform development

The well-known displacement-based creep damage algorithm will be adopted here directly [31], which were used and reported, for example, research [32] by Richard Hall.

The main further work is the calculation of the stiffness matrix for the grain boundary element and the integration of the grain boundary element, parallel to that for grain element.

3. Materials

1. P91 high Cr alloy is used in this development of creep cavity fracture model and the associated creep cavity nucleation model and creep cavity growth model [12, 31]. The experimental cavity histogram data was taken from publication [21].
2. ASME Grade 91 (9Cr-1Mo-V-Nb) high Cr alloy is used in the investigation of the trend of creep cavity fracture lifetime coefficient U' . The creep data sheets of creep fracture time under different stress and temperature on this alloy is taken from publication [20].
3. CB8 high Cr alloy is used in the investigation of creep cavity fracture lifetime over a wider stress range. The experimental creep cavitation data and histogram (in the form of graphs) were taken from Ref. [33].
4. Copper-antimony alloy is used for the demonstration of the mesoscopic composite creep cavity damage simulation. The property of copper-antimony alloy at 823 K [24].

The parameters for the grain boundary cavity model is $\tilde{D}_{gb} = 10^{-14} mm^5 N^{-1} s^{-1}$, $a_p = 2 \times 10^2 mm^{-2} s^{-1}$, and $b_p = 1$. The power law creep is used to describe the creep mechanism of the grain part.

The material parameters of copper power law for grain [24] are (400–700°C): A : $38.8 \text{ MPa}^{-n} \text{ s}^{-m-1}$, Q : 197 KJmol^{-1} , n :4.8, and m :0.

A 1 mm^2 square geometry is chosen, 20 grains and 60 grain boundary were meshed by 909 triangle plane strain element; 152 interface elements, using Neper free software [34]. A finer mesh would be desirable; however, it is a compromise to accept this size to proceed.

A tensile load of 10 MPa was applied uniformly on the top side; and the left side and the bottom side was pinned in X direction and Y direction, respectively.

4. Results

4.1 The minimum creep strain rate over a wide range of stress levels for P91 high Cr alloy

The specific value of $q = 2$ of the modified hyperbolic sine law was obtained through trial and error method. The results are summarily shown in **Figure 2**, where it is clearly shown that the Xu's modified hyperbolic sine law is the best.

4.2 Creep cavity fracture model

4.2.1 The determination of the creep cavitation coefficients

The obtained creep cavitation coefficients were obtained and shown in **Table 3**, and their application to predict the cavity probability density size distribution is shown in **Figure 3** [12].

Based on the obtained values of creep cavity coefficients, the creep cavity nucleation model, the creep cavity growth model, and creep cavity fracture model

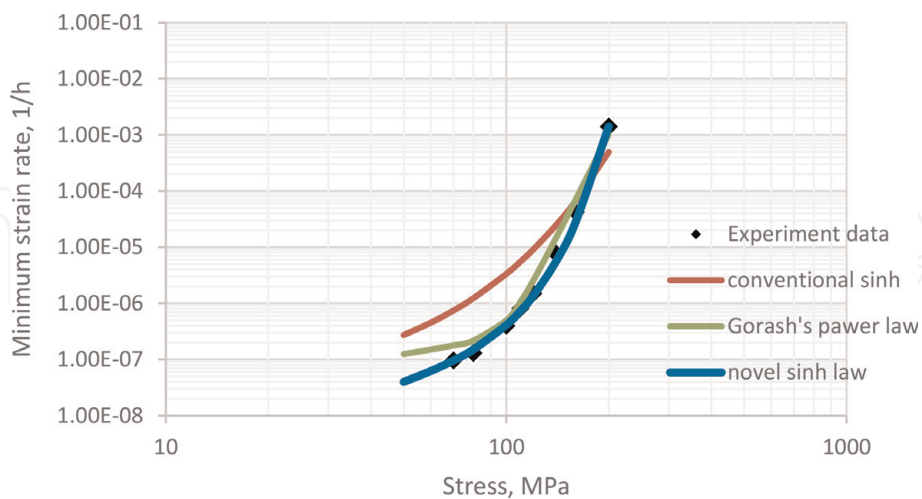


Figure 2.
 The comparison of the modeling of minimum creep strain rate and stress level [12].

A_1	A_2	α	β	γ
6.66E-18	0.019246	1	2	1

Table 3.
 The creep cavitation constants for P91 [12].

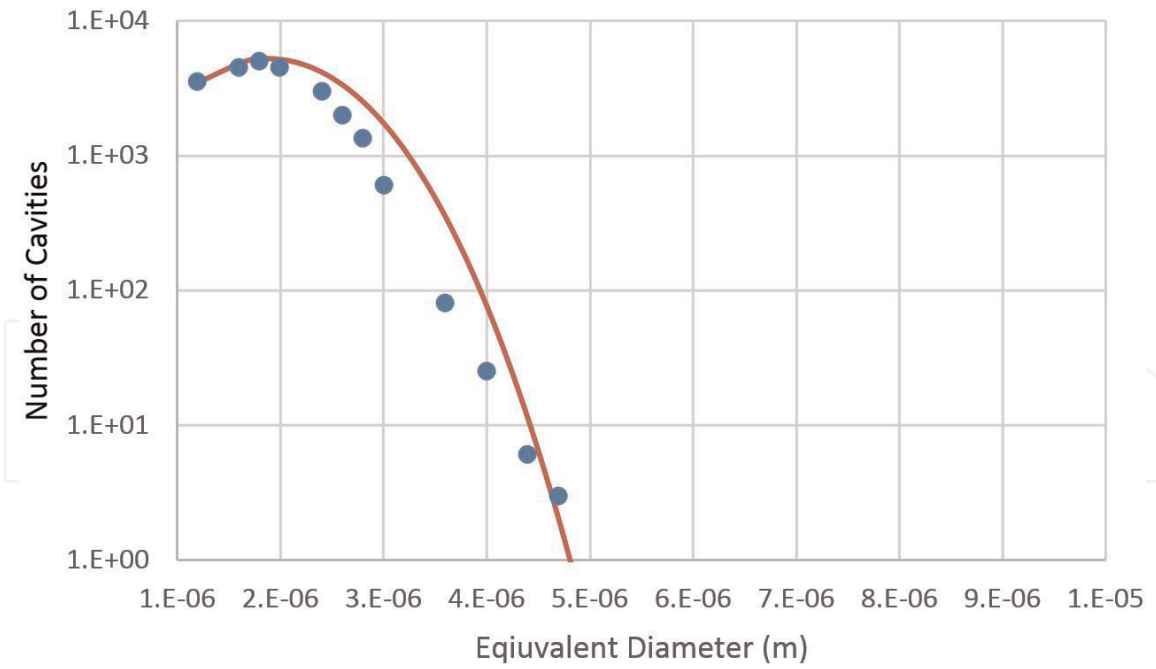


Figure 3.
The comparison of cavity size probability density function for P91, experimental data from ref [22] and only sample points used [12].

Cavity Number Density and Time

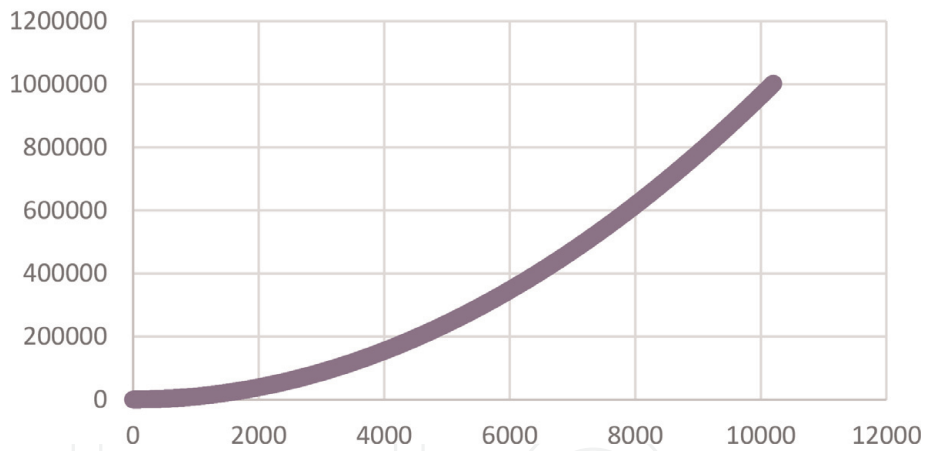


Figure 4.
The predicted number of cavity with time.

Cavity Growth R

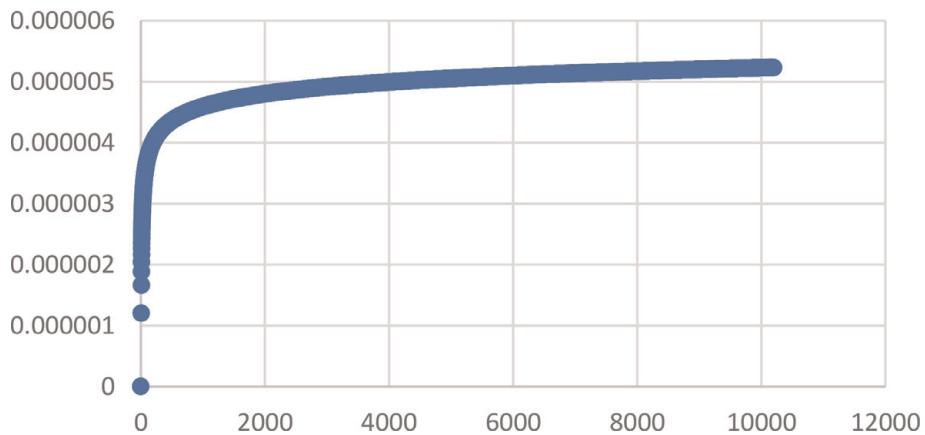


Figure 5.
The predicted cavity growth with time.

Cavity Rupture Variable and Time

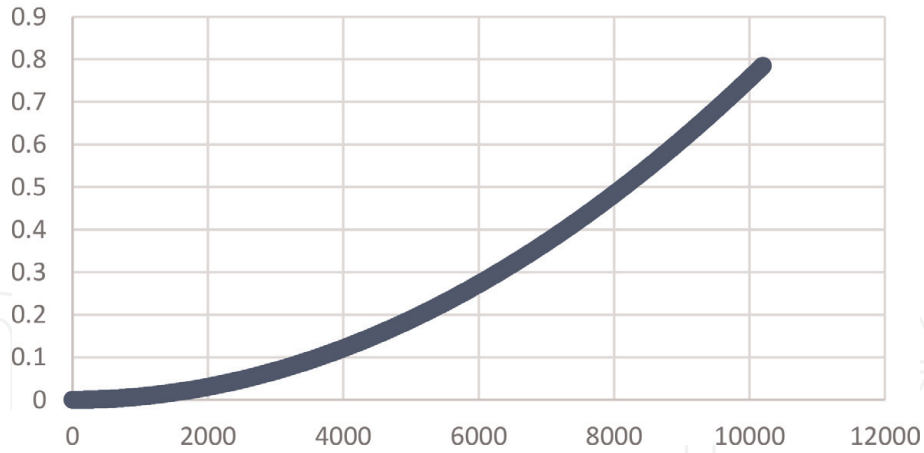


Figure 6.
 The predicted caviated area along grain boundary with time.

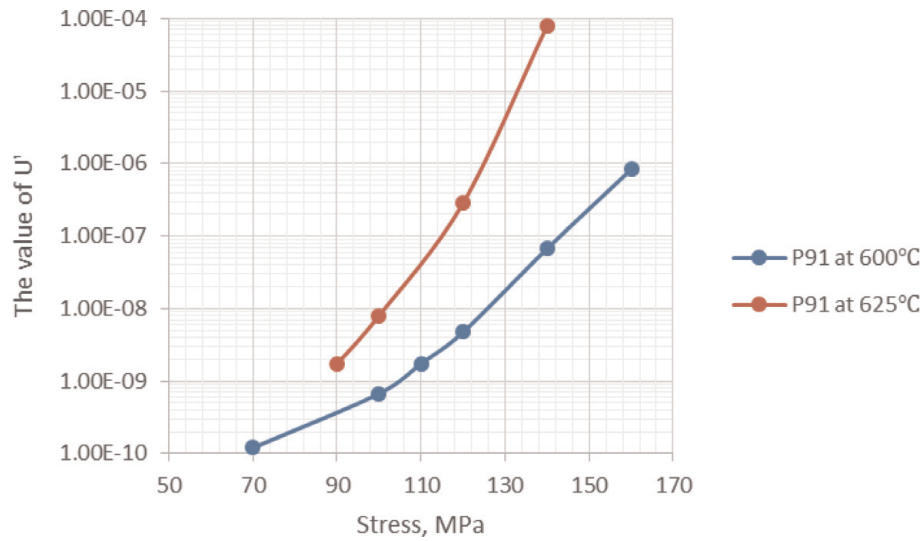


Figure 7.
 The trend of the values of U' under different stresses and temperatures [12].

Inverse U' and Stress

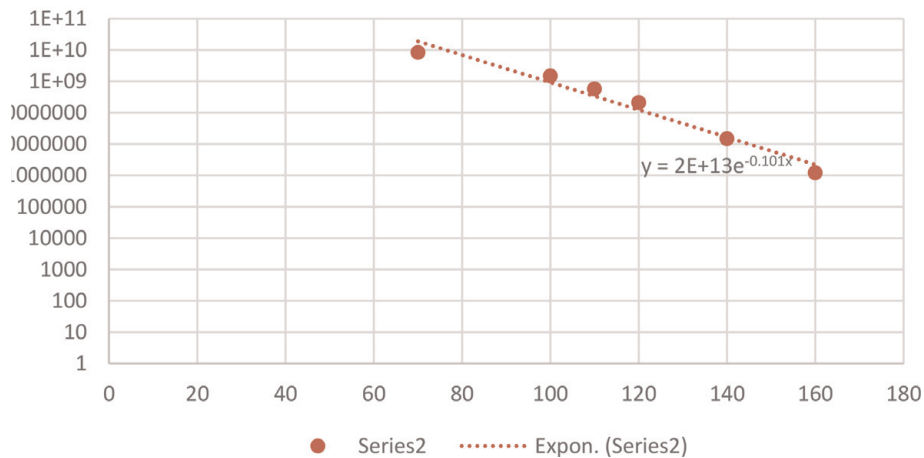


Figure 8.
 Inverse U' and stress level for P91 at 600°C.

are also obtained, respectively. The predicted relationships of the number of cavity, the creep cavity growth, and creep damage variable with time are shown in **Figures 4–6**, respectively.

4.2.2 Trend of creep fracture lifetime coefficient U'

Based creep data sheets of creep fracture time under different stress and temperature on typical ASME Grade 91(9Cr-1Mo-V-Nb) steel [14], the value of U' was calculated and graphically shown in **Figure 7**. Furthermore, the inverse U' and stress level for P91 is obtained and shown in **Figures 8 and 9**, respectively.

4.2.3 Creep cavity fracture lifetime prediction over a stress range

Using the simplified and approximate method described in Section 2.2.3, the obtained values for the cavity nucleation coefficient and cavity growth coefficient are shown in **Table 4**.

Based on Equation (12), the creep lifetime at 120 MPa is predicted to be 44,845 hours, and it is 87% of the actual experimental lifetime of 51,406 (hours).

4.3 Mesoscopic composite model of the simulation of creep cavity damage and fracture

The flow diagram structure is shown in **Figure 10**; the FE model of the polycrystalline case is shown in **Figure 11** [31].

At the time of 78.9 hours, there were seven grain boundary elements that failed. If that is deemed as creep fracture time, then it agrees with the majority of all

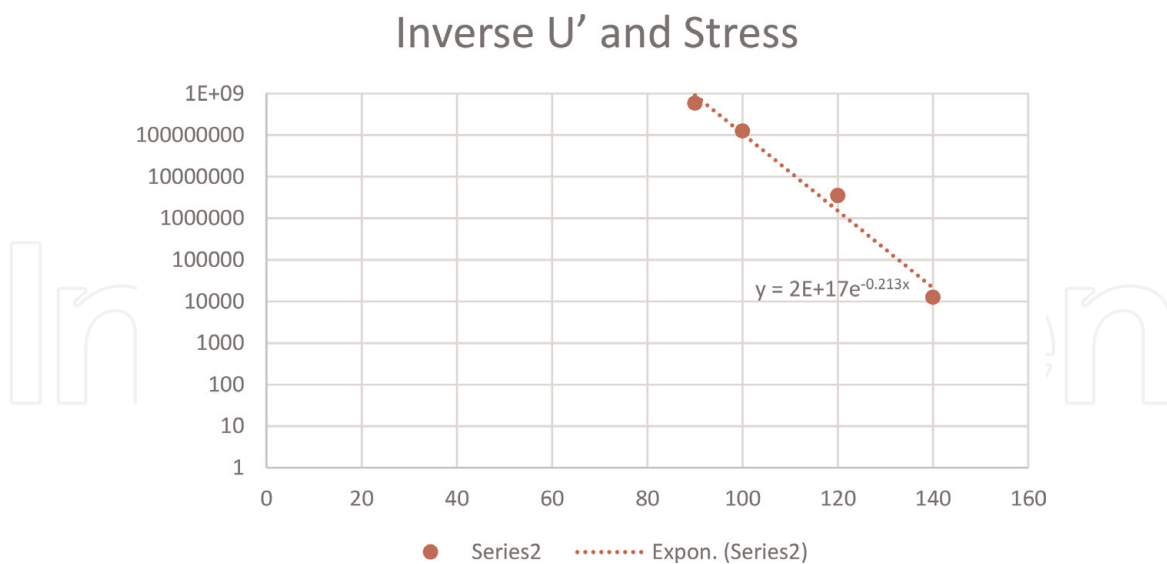


Figure 9.
Inverse U' and stress level for P91 at 625°C.

Stress	A_1	A_2	Lifetime (hours)
180 MPa	1.73E-17	9.397e-8	2825 (experiment)
120 MPa	7.04E-17	8.04e-10	51406 (experiment) 44845 (predicted)

Table 4.
The values of nucleation coefficient and growth coefficient and lifetime prediction.

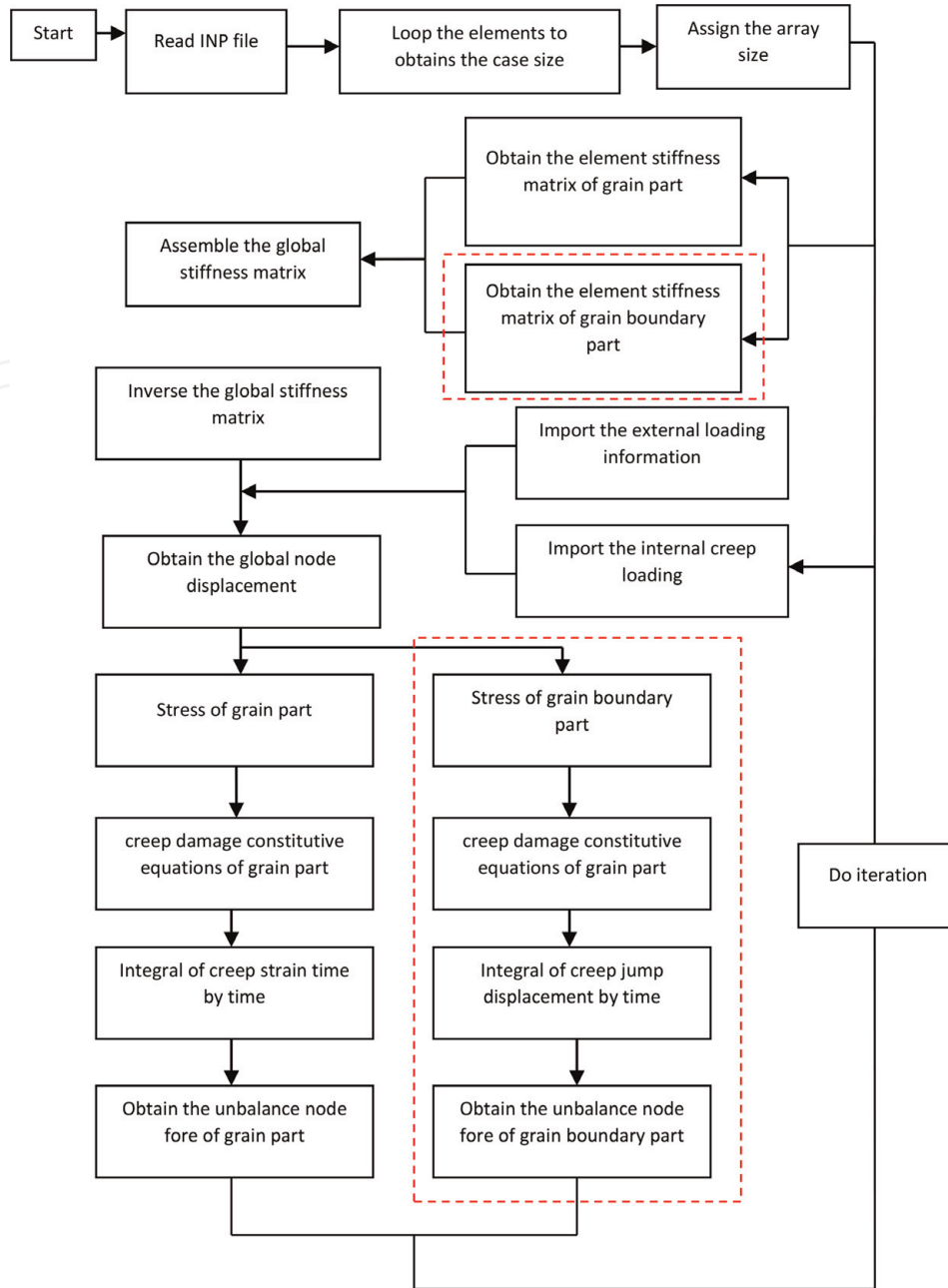


Figure 10.
 The flow diagram structure [31].

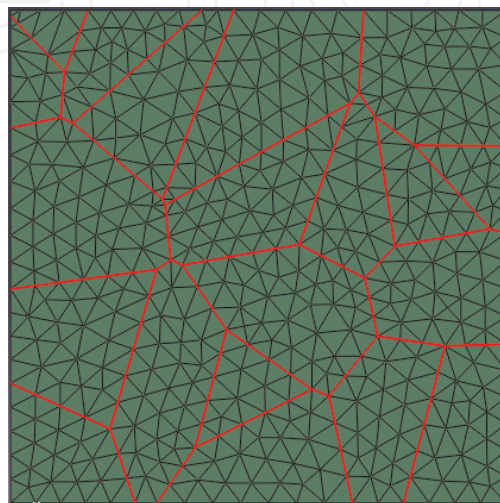


Figure 11.
 The FE model of the polycrystalline case study [31].

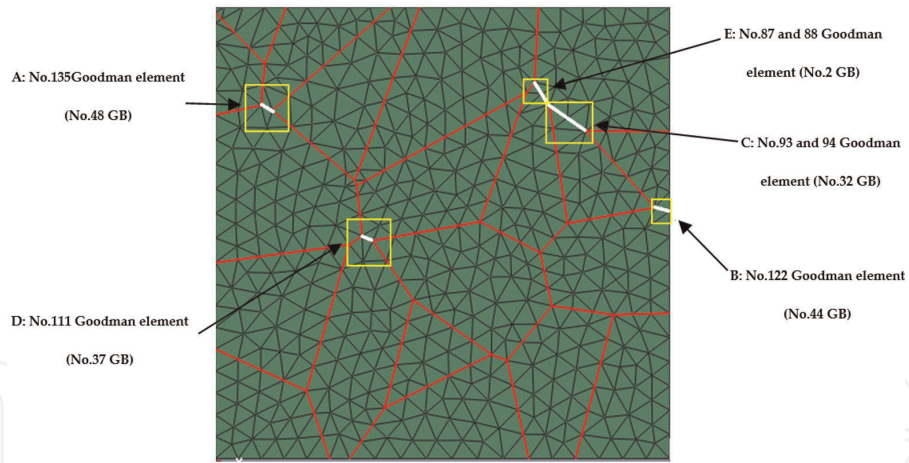


Figure 12.
The location of the first seven failed grain boundary elements [31].

Position	Oritantion Angle (Normal direction)	Element NO.	Time (Unit:hour)	Step
A	65.26084	48	23.55	12003387
B	76.16616	122	65.55	33246192
C	54.01357	93	68.48	34728834
D	54.01357	94	68.48	34728856
E	65.41204	111	70.69	35848560
F	146.3127	87	78.90	39987506
G	146.3128	88	78.90	39987517

Table 5.
The sequence and time of fracture [31].

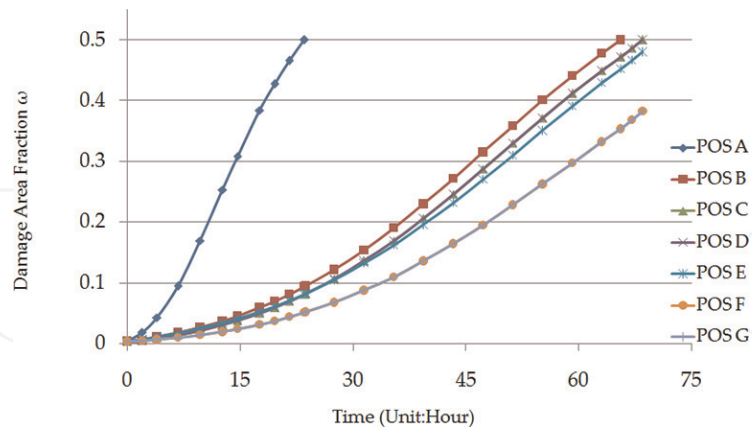


Figure 13.
The damage evolution with time of the seven failed grain boundary elements [31].

uni-axial creep tests conducted [9]: In uniaxial test, one specimen is fractured at 16.6, 17.9, and 58.3 hours, respectively. It is worthy to mention that the simulation was conducted for plane strain case; hence a longer lifetime at the same applied stress is expected.

The location, the sequence of fracture, and the time of fracture of grain boundary element are shown in **Figure 12** and **Table 5**, respectively. The creep cavity damage evolution with time of the first seven failed grain boundary elements is

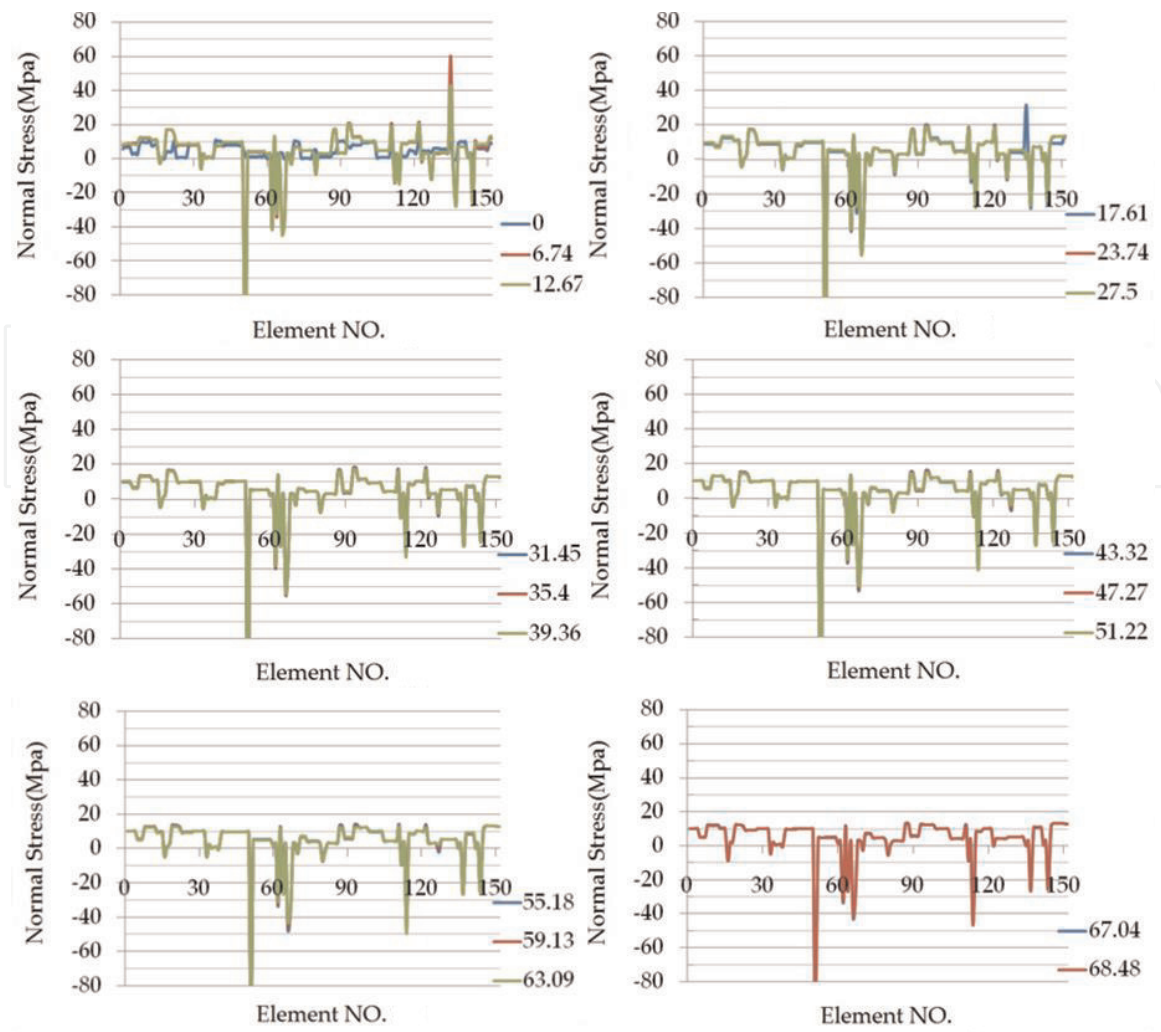


Figure 14.
 The evolution of normal stress with time [31].

shown in **Figure 13**. The whole all normal stress evolution and the creep cavity damage evolution are shown in **Figures 14** and **15**, respectively.

5. Discussion

5.1 The minimum creep strain rate over a wide range of stress levels for P91 high Cr alloy

The results shown in **Figure 2** clearly demonstrated that Xu's modified hyperbolic sine law is the best for the P91 high Cr alloy over a wider range of stress levels.

It is pointed out that the introduction of σ^q into the normal hyperbolic sine function, purposely, offers a capability to depict a wider range of curvatures between the minimum creep strain rate and stress level.

Furthermore, the value $q = 2$ found here for P91 is in similar order to those found for low Cr alloy [12] and for P92 [35]. It is worth to research any profound reason for this similarity.

It is reasonable to propose that, due to generic mathematical property (feature), the application of Xu's modified hyperbolic sine law should be further explored, particularly for a wider range of stress level cases.

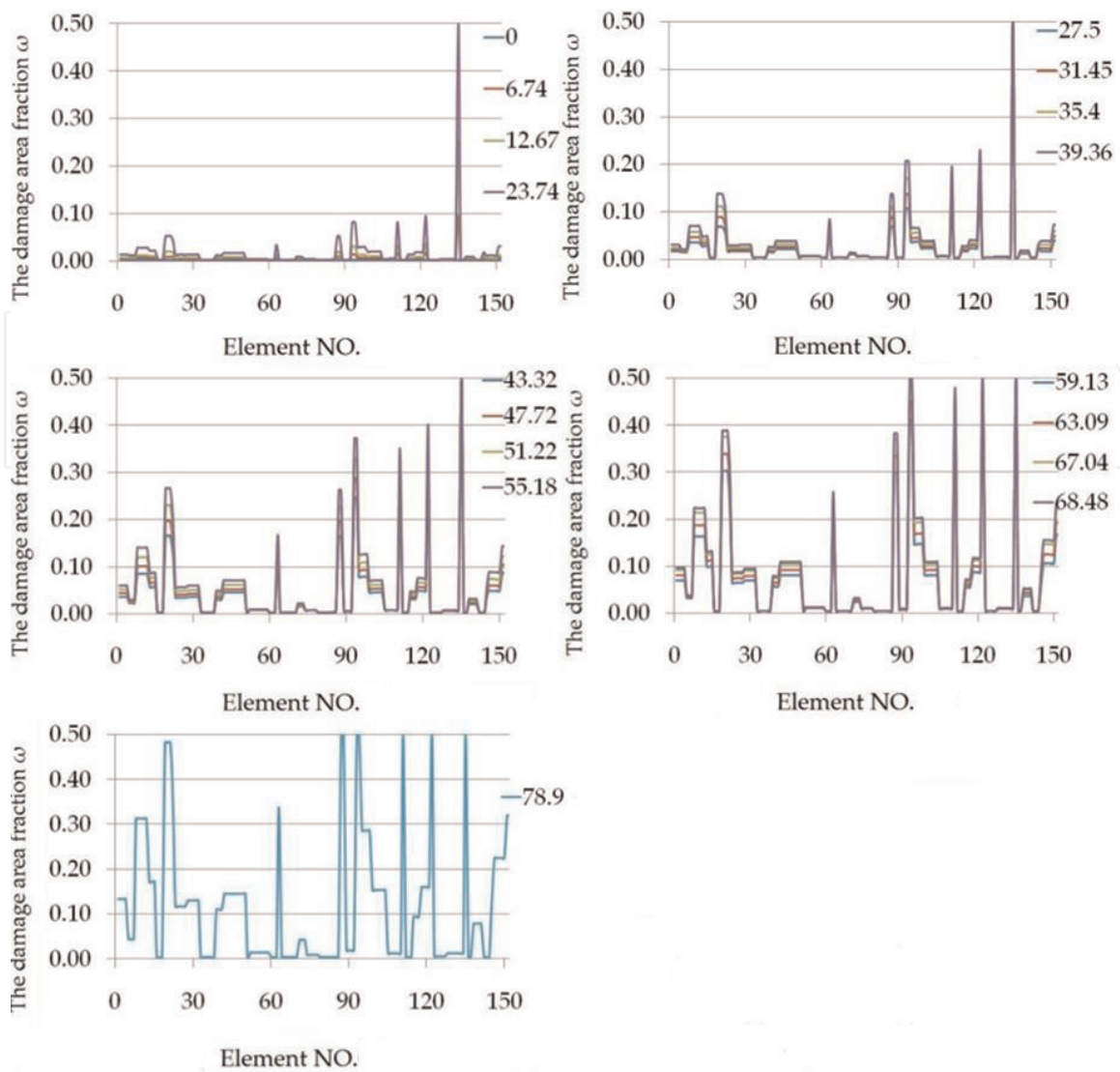


Figure 15.
The damage evolution with time [31].

5.2 Creep cavity fracture model

5.2.1 The determination of the creep cavitation coefficients

A set of creep cavitation model and creep cavity growth model were calibrated using the more representative X-ray synchrotron cavitation data. The predicted cavity size probability density is very close to the experimental measured one, indicated by **Figure 3**, and it can be concluded that the quality of creep cavitation models are good. Hence their application should also be reliable [12].

The predicted relationships of the number of cavity, the creep cavity growth, and creep damage variable with time can provide the insight of the evolution of the complex creep cavity damage process, and its use will lead to a clear and definite answers on (1) how to present creep cavity damage and (2) how to quantify it.

The obtained *explicit creep cavity damage fracture model can be used for creep lifetime prediction and possible extrapolation.*

5.2.2 Trend of creep fracture lifetime coefficient U'

The creep lifetime coefficient U' is introduced in theoretically based cavitation nucleation, growth, and coalescence along the grain boundary. A clear trend shown

from the experimental data, in **Figure 7**, indicated that such creep cavity damage/fracture modeling is scientifically sound and numerically reliable; hence it can be used for creep life time prediction and possible extrapolation.

Furthermore, theoretically, creep lifetime coefficient and lifetime, in log–log scale, is a linear relationship; and the experimental data strongly support that as shown in **Figures 8** and **9**. Hence the trend revealed by experimental data in **Figures 8** and **9** could be used for lifetime prediction and very promising for lifetime extrapolation.

5.2.3 Creep cavity fracture lifetime prediction over a stress range

The excellent agreement (87%) between the predicted creep lifetime and experimental measured one proved the reliability of creep lifetime prediction.

It needs to be reported here [33] that the stress of 180 MPa is of the high stress level and the stress of 120 MPa is of the lower stress level. Hence, the above excellent agreement is actually achieved between two stress levels. There is no stress breakdown phenomenon in this approach; actually, the stress-dependent effects will be taken into account by the values of the creep cavitation coefficients.

The success is underpinned by both the correct mathematical model and the direct using the most presentative cavitation data.

Furthermore, the creep cavitation modeling approach reported here should be generic and can be used for any other cavitation controlled damage and fracture problems such as ductile fracture, fatigue fracture, and creep and fatigue combined fracture.

5.3 Mesoscopic composite model of the simulation of creep cavity damage and fracture

1. The concept of mesoscopic composite-type approach of modeling creep damage model at grain boundary level has been proposed and developed.
2. In this development, in the conventional nonlinear creep damage analysis framework, the only new thing that needs to be added is the grain boundary element.
3. The existing interface element has been chosen and used here.
4. The predicted creep lifetime is in very good agreement with experimental observation.
5. The demonstrative case study reveals its full potential for providing the detailed information at the right size level, and it is anticipated to be widely used in the future.
6. There is an urgent need for the development of creep damage constitutive equations for grain and grain boundary, respectively; in turn, it demands the characterization of the grain and grain boundary separately.
7. Further development work to develop a three-dimensional version.

6. Conclusion

Modeling of creep deformation and creep fracture is very challenging. However, research work report here has made some progress. These progress and suggestions

for future work are presented as:

1. A modified hyperbolic sine function was proposed, and suitability for a wider range of stresses is demonstrated. Its successful applications to both low Cr alloy and high Cr alloy merit it to be tried to other alloys. It is worth to research to find any material scientific reasons for the similar magnitude of the q among different alloys.
2. A new creep cavity fracture model was proposed and developed based on the cavity nucleation, growth, and coalesce at grain boundary using the cavitation data from X-ray synchrotron investigation.
3. The creep cavity fracture lifetime coefficient U' can be experimentally produced, and it can be used for lifetime prediction and extrapolation.
4. Creep cavity fracture lifetime prediction works very well over a stress range, and there is no stress breakdown in this model.
5. Research work on the stress state's effect on the cavitation should be pursued in the future.
6. Furthermore, the creep cavitation modeling approach reported here should be generic and can be used for any other cavitation controlled damage and fracture problems such as ductile fracture, fatigue fracture, creep, and fatigue combined fracture.
7. A mesoscopic creep deformation and creep damage model concept was proposed and preliminarily realized in a plane stress version; its potential for providing the right size has been demonstrated.
8. Parallel to the development of 3D computational platform, there is a great need for the development of creep damage constitutive equations for grain and grain boundary separately.

Acknowledgements

QX is grateful for the award of the Santander postgraduate mobility scholarship 2016 and 2017, respectively, which partially funded the field trip of Mr. Xin Yang in 2016 to Japan and Mr. JiaDa Tu in 2018 to China, respectively. It is also acknowledged that some work reported here were taken from previous publications [12, 31] where Dr. Xin Yang and Mr. Jiada Tu did contribute in the original production of these two papers, respectively.

Conflict of interest

The authors declare that there is no conflict interest.

IntechOpen

IntechOpen

Author details

Qiang Xu* and Zhongyu Lu
School of Computing and Engineering, The University of Huddersfield,
Huddersfield, West Yorkshire, UK

*Address all correspondence to: q.xu2@hud.ac.uk

IntechOpen

© 2019 The Author(s). Licensee IntechOpen. This chapter is distributed under the terms of the Creative Commons Attribution License (<http://creativecommons.org/licenses/by/3.0>), which permits unrestricted use, distribution, and reproduction in any medium, provided the original work is properly cited. 

References

- [1] Riedel H. Fracture at High Temperatures. Springer Verlag; 1987
- [2] Kassner ME, Hayesb TA. Creep cavitation in metals. *International Journal of Plasticity*. 2003;**19**:1715-1748
- [3] Ennis PJ, Zielinska-lipiec A, Wachter O, Czyrska-filemonowicz A. Microstructural stability and creep rupture strength of the martensitic steel P92 for advanced power plant. *Acta Materialia*. 1997;**45**(12):4901-4907
- [4] Lee JS, Armakia HG, Maruyamab K, Murakic T, Asahic H. Causes of breakdown of creep strength in 9Cr–1.8W–0.5Mo–VNb steel. *Materials Science and Engineering*. 2006;**428**:270-275
- [5] Grades EA. Development of a creep-damage model for non-isothermal long-term strength analysis of high-temperature components operating in a wide stress range, Zentrum für Ingenieurwissenschaften der Martin-Luther-Universität at Halle-Wittenberg; 2008
- [6] Parker J. In-service behavior of creep strength enhanced ferritic steels grade 91 and grade 92 – Part 1 parent metal. *International Journal of Pressure Vessels and Piping*. 2013;**101**:30-36
- [7] Miannay D. Time-Dependent Fracture Mechanics. France: Springer; 2001
- [8] Dyson B. Use of CDM in materials modelling and component creep life prediction. *International Journal of Pressure Vessels and Piping*. 1983;**122**: 281-296
- [9] Yin Y, Faulkner RG, Morris PF, Clarke PD. Modelling and experimental studies of alternative heat treatments in steel 92 to optimise long term stress rupture properties. *Energy Materials*. 2008;**3**:232-242
- [10] Yang X, Xu Q, Lu ZY. The development and validation of the creep damage constitutive equations for P91 alloy. In: *Proceedings of the 2013 World congress in computer science and computer engineering and application*. CSREA Press; 2013. pp. 121–127. ISBN: 1-60132-238-0
- [11] Basirat M, Shrestha T, Potirniche GP, Charit I, Rink K. A study of the creep behavior of modified 9Cr-1Mo steel using continuum-damage modeling. *International Journal of Plasticity*. 2012;**37**:95-107
- [12] Xu Q, Yang X, Lu ZY. On the development of creep damage constitutive equations: a modified hyperbolic sine law for minimum creep strain rate and stress and creep fracture criteria based on cavity area fraction along grain boundaries. *Materials at High temperatures*; **34**(5–6):323-332. DOI: 10.1080/09693409.2017.1388603
- [13] Xu Q, Hayhurst DR. The evaluation of high-stress creep ductility for 316 stainless steel at 550 °C by extrapolation of constitutive equations derived for lower stress levels. *International Journal of Pressure Vessels and Piping*. 2003; **80**(10):689-694. ISSN: 0308-0161
- [14] Xu Q. Development of constitutive equations for creep damage behaviour under multi-axial states of stress. In: *Advances in Mechanical Behaviour, Plasticity and Damage*. London, UK: Elsevier; 2000. pp. 1375-1382. ISBN: 978-0-08-042815-4
- [15] Xu Q. Creep damage constitutive equations for multi-axial states of stress for 0.5Cr0.5Mo0.25V ferritic steel at 590°C. *Theoretical and Applied Fracture Mechanics*. 2001;**36**(2):99-107. ISSN: 0167-8442
- [16] Xu Q. The development of phenomenological multi-axial isotropic

- creep damage constitutive equations. In: *Mechanics and Material Engineering for Science and Experiments*. London, UK: Science Press; 2001. pp. 457-460. ISBN: 1-880132-79-6
- [17] Xu Q. The development of validation methodology of multi-axial creep damage constitutive equations and its application to 0.5Cr0.5Mo0.25V ferritic steel at 590°C. *Nuclear Engineering and Design*. 2004;**228**(1–3): 97-106. ISSN: 0029-5493
- [18] Wen JF, Tu SD. A multiaxial creep-damage model for creep crack growth considering cavity growth and microcrack interaction. *Engineering Fracture Mechanics*. 2014;**123**:197-210
- [19] Xu Q, Lu ZY, Wang X. Damage modelling: The current state and the latest progress on the developing of creep damage constitutive equations for high Cr steels. In: 6th International 'HIDA' Conference: Life/Defect Assessment & Failures in High Temperature Plant; 2–4 December 2013, Nagasaki, Japan. Surrey, UK: European Technology Development Limited; 2013
- [20] Creep and rupture data of heat resistant steels, National Institute for Materials Science (NIMS). Available from: http://smds.nims.go.jp/creep/index_en.html
- [21] Sket F, Dzieciol K, Borbely A, Kaysser-Pyzalla AR, Maile K, Scheck R. Microtomography investigation of damage in E911 steel after long-term creep. *Materials Science and Engineering A*. 2010;**528**:103-111
- [22] Renversade L, Ruoff H, Maile K, Sket F, Borbely A. Microtomographic assessment of damage in P91 and E911 after long-term creep. *International Journal of Materials Research*. 2014;**105**: 621-627
- [23] Vöse M, Otto F, Fedelich B, Eggeler G. Micromechanical investigations and modeling of a copper–antimony-alloy under creep conditions. *Mechanics of Materials*. 2014;**69**(1):41-62
- [24] Vöse M, Fedelich B, Otto F, Eggeler G. Micromechanical modeling of creep damage in a copper-antimony alloy. *Procedia Materials Science*. 2014;**3**:21-26
- [25] Dyson BF. Continuous cavity nucleation and creep fracture. *Scripta Metallurgica*. 1983;**17**:31-37
- [26] Bower AF. *Applied Mechanics of Solids*. Oxford, UK: Taylor & Francis Group, LLC; 2010
- [27] Dyson BF. Constraints on diffusional cavity growth rates. *Metal Science*. 1976;**10**:349-353
- [28] Ashby MF. Boundary defects and atomistic aspects of boundary sliding and diffusional creep. *Surface Science*. 1972;**31**:498-542
- [29] Cocks ACF, Ashby MF. On creep fracture by void growth. *Progress in Materials Science*. 1982;**27**:189-244
- [30] Vöse M, Fedelich B, Otto F, Owen J. A simplified model for creep induced grain boundary cavitation validated by multiple cavity growth simulations. *Computational Materials Science*. 2012;**58**:201-213
- [31] Xu Q, Tu JD, Lu ZY. Development of the FE In-house procedure for creep damage simulation at grain boundary level. *Metals*. 2019;**9**(6):656. DOI: 10.3390/met9060656
- [32] Hall R. Development of continuum damage mechanics models to predict the creep deformation and failure of high temperature structures [PhD thesis]. The University of Sheffield; 1990
- [33] Gupta C, Toda H, Schlacher C, Adachi Y, Mayr P, Sommitsch C, et al.

Study of creep cavitation behavior in tempered martensitic steel using synchrotron micro-tomography and serial sectioning techniques. *Materials Science and Engineering A*. 2013;**564**: 525-538

[34] Quey RP, Dawson P, Barbe B. Large scale 3D random polycrystals for the finite element method: Generation, meshing and remeshing. *Computer Methods in Applied Mechanics and Engineering*. 2011;**200**(2011):1729-1745

[35] Zheng XM, Xu Q, Lu ZY. The development of creep damage constitutive equations for high Cr steel: Further application of the modified hyperbolic sine law for the minimum creep strain rate over a wider range of stress level and the creep cavity fracture model based on the cavity area fraction along grain boundaries. *Materials at High Temperatures*. 2019

IntechOpen